ELSEVIER

Nuclear Physics A 645 (1999) 191-202

NUCLEAR PHYSICS A

Time-decay history of normal-deformation high-spin states in ^{193,194}Hg

L. Weissman [a], R.H. Mayer [b,1], N. Benczer-Koller [b], C. Broude [c], J.A. Cizewski [b], M. Hass [c], J. Holden [b], R.V.F. Janssens [d], G. Kumbartzki [b], T. Lauritsen [d], I.Y. Lee [e], A.O. Macchiavelli [e], N. Matt [b,2], D.P. McNabb [b,3], M. Satteson [b,4]

[a] *Katholieke Universiteit, Leuven, Belgium*
[b] *Rutgers University, New Brunswick, NJ 08903, USA*
[c] *Weizmann Institute of Science, Rehovot 76100, Israel*
[d] *Argonne National Laboratory, Argonne, IL 60439, USA*
[e] *Lawrence Berkeley Laboratory, Berkeley, CA 94720, USA*

Received 21 September 1998; accepted 6 November 1998

Abstract

The time evolution of the decay of high-spin, normal deformed structures in ^{193,194}Hg was studied by measuring, in the Gammasphere array, the Doppler shift attenuation of selected transitions depopulating various bands. The data suggest that a fraction of states feeding selective yrast levels is non-collective in nature and show resemblance to $A = 150$ nuclei where shape polarizing effects have been linked to particles occupying high-j orbitals. © 1999 Elsevier Science B.V.

PACS: 21.10.Ky; 21.10.Tg; 27.80.+w

1. Introduction

The neutron deficient Hg isotopes have been the subject of intense investigations at new generation large γ-ray detector arrays. This interest was fueled mostly by the discovery of superdeformed (SD) bands in this mass region [1]. Properties of yrast and ex-

---

[1] Present address: School of Chemical Engineering, Purdue University, West Lafayette, IN 47907, USA.
[2] Present address: Microsoft Corporation, Redmond WA 98052-6399, USA.
[3] Present address: Lawrence Livermore National Laboratory, Livermore, CA 94550, USA.
[4] Present address: Interventional Innovations, St. Paul, MN 55113, USA.

PII S0375-9474(98)00604-6

cited superdeformed bands such as transition energies, moments of inertia and transition quadrupole moments Q_t have been determined for several Hg isotopes, demonstrating the fast decay times and collective character of superdeformed levels [1–5]. However, little information exists as to decay times of yrast and near-yrast, normal-deformed level structures of Hg nuclei even though level schemes extending to very high spins have been established [6–9]. These nuclei have been characterized by an oblate, collective shape at low and moderate spin and, as such, provide an ideal testing ground for cranked shell model calculations in the limit of oblate deformation. Above a spin of $\sim 20\hbar$, however, structural changes have been reported recently [10–12] in several Hg isotopes, illustrating the polarizing effects brought about by particle alignments under the stress of rotation. Lifetime information was obtained for dipole bands in ^{192}Hg [13]. However, time-decay history, which probes the total decay time in a particular γ cascade, can provide additional valuable information concerning these issues and is the subject of this publication.

The present results were obtained in an experiment carried out on the Gammasphere array [14]. The experiment was primarily designed to measure magnetic moments of high-spin states and thus required a special, multi-element, target [15]. This target had a layer of ^{150}Nd deposited on a gadolinium foil. However, the Nd layer did not adhere to the gadolinium resulting in the formation of a gap between these two layers. The resulting gap in the target, nevertheless, could be exploited for Doppler attenuation measurements to yield information on the time-decay histories of high spin levels at normal deformation in ^{193,194}Hg.

2. Experiment

The reactions ^{150}Nd(^{48}Ca, 5n and 4n) were used to populate high-spin states in ^{193}Hg and ^{194}Hg. The 203 MeV beam was provided by the 88" Cyclotron of the Lawrence Berkeley National Laboratory. The γ rays of interest were detected with the Phase I implementation of the Gammasphere array, which at that time contained 64 Compton suppressed detectors. The event trigger required at least three γ rays. A total of 5×10^8 events was analyzed.

The target was actually prepared by pressing together a 1 mg/cm^2 isotopically enriched ^{150}Nd foil with 200 μg/cm^2 of gold evaporated on one side and a ferromagnetic, 2.15 mg/cm^2, gadolinium foil faced by a 200 μg/cm^2 gold cover and backed by a 25 mg/cm^2 thick gold layer. Another 200 μg/cm^2 gold layer was evaporated on the upstream surface of the ^{150}Nd in order to prevent oxidation.

3. Gap determination – ^{150}Nd analysis

The width of the gap in the target was determined from an analysis of the partially Doppler shifted, 409-keV, $8^+ \rightarrow 6^+$, yrast transition in ^{150}Nd. This transition is present

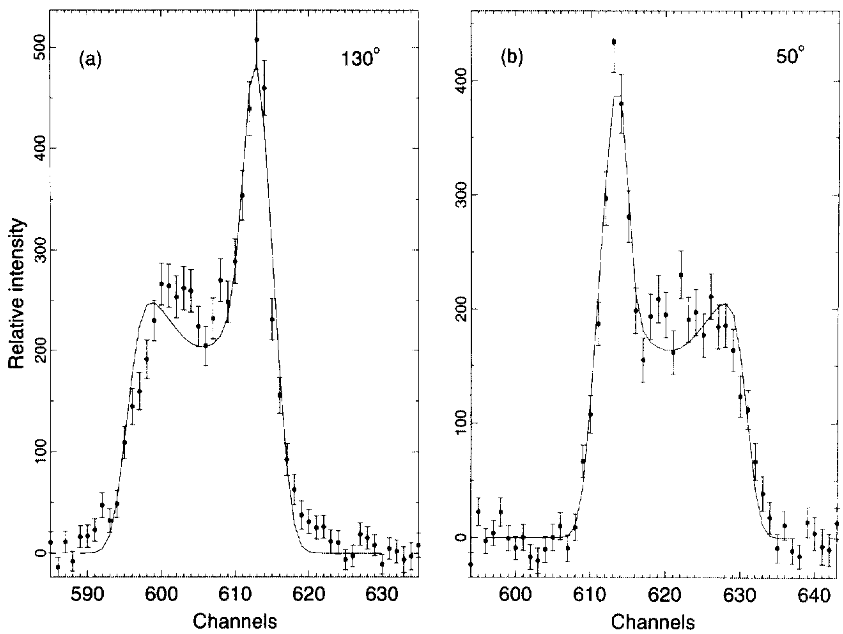

Fig. 1. Gamma-ray spectra in coincidence with the 251 keV, $4^+ \to 2^+$, transition in ^{150}Nd as recorded by detectors at 130° (a) and 50° (b) showing the 409-keV, $8^+ \to 6^+$, transition together with fits to the line shapes. Background contributions have been subtracted.

in the spectra as a result of Coulomb excitation of the ^{150}Nd by the ^{48}Ca beam.

To enhance events associated with Coulomb excitation, a low multiplicity cut on a fold parameter was imposed during the sorting of the data. The fold parameter was defined as the sum of the number of Compton-suppressed and unsuppressed Ge detectors as well as sole anti-Compton shields when no photons were recorded in the enclosed Ge detectors. Events with fold $\leqslant 6$ were "unpacked" using the sorting method described in Ref. [16] and random coincidences were subtracted. Double-gated coincidence spectra requiring one of the five lowest transitions in the yrast band of ^{150}Nd and the $4^+ \to 2^+$, 251 keV γ-ray were created for the detectors located in rings at 50° and 130° with respect to the beam direction. Fig. 1 shows parts of these spectra after subtraction of background by the method described in Ref. [17]. The gating conditions lead to very clean spectra and the $8^+ \to 6^+$ transition in ^{150}Nd clearly shows stopped and Doppler-shifted decay components.

This transition provides an estimate of the size of the gap between the ^{150}Nd foil and the gadolinium layer since, except for the gap, the parameters which determine the Doppler broadened lineshape, such as the B(E2) values of the ground-state band and the meanlife of the 8^+ level, $\tau(8^+) = 6.3(0.5)$ ps, are known [18]. A computer program was developed to calculate the shape of the line including the effect of the recoil velocity distribution, using differential cross sections from a Coulomb excitation code; the energy loss of the recoils in the various materials was calculated from the stopping powers provided by the TRIM95 code [19]. Since the ^{48}Ca energy is above the Coulomb barrier, an adjustment was made to the differential cross sections: it was assumed that the Coulomb excitation cross section drops to zero at some angle below the grazing angle of 95°. This assumption is justified from experimental data regarding Coulomb excitation near the barrier [20]. The cutoff angle was determined to be 75° by adjusting the high velocity edge of the observed line shapes to the calculated line shapes.

The determination of the average recoil velocity for the Hg nuclei, produced in the fusion-evaporation reaction, was made from the measurement of the Doppler shifts seen for superdeformed transitions, practically all of which decay inside the gap. This velocity, $v/c = 0.019$, agrees with that calculated from the reaction kinematics and the target composition.

A single-valued gap was assumed in the lineshape fitting procedure. This assumption was tested in the following manner: for a given meanlife, lineshapes were computed and numerically integrated for a gap with a uniformly distributed width. The spread in gap is expressed as a percentage of the mean gap: for example, a 50% spread means that the gap varies uniformly between 0.5 and 1.5 times the mean value of the gap. From these integrated lineshapes, stopped fractions F = [stopped/(stopped + flight)] were extracted. Stopped fractions were also calculated for the case of (HI,xn) reactions, where the velocity is essentially single valued and the F values can be calculated analytically by integrating the exponential decay between a minimum and maximum gap. The computed F values corresponding to various gaps are presented for both the Coulomb excitation (Fig. 2a) and the (HI,xn) cases (Fig. 2b). From the calculations it can be concluded that for a $\pm 50\%$ range around the mean gap, the absolute effect of a gap spread is small compared to other errors. Furthermore, the present analysis uses the ^{150}Nd Coulomb excitation data to extract the value of the gap and then uses this value in the analysis of the time-decay history of transitions in ^{193,194}Hg. Hence, as Fig. 2 demonstrates, a possible gap spread influences the extracted information only to the extent of the different functional behavior of the two reactions.

The width of the gap, 46(5) μm, was obtained from the best fit (χ^2 minimization) of the spectra with the calculated lineshapes. The corresponding transit time through the gap is 8.1 ps. The fits to the data are shown in Fig. 1.

It should be emphasized that any uncertainty in the fitting procedure that determines the gap size does not affect the conclusions of the experiment as the results describe *relative* time behavior of various bands in both ^{193,194}Hg. It is also important to note that the main feature of the present technique consists in determining the target-stopper distance *simultaneously* by another nuclear reaction, using the same beam and the same target with its own microscopic structure and inhomogeneity. As such, it may provide an important addition to the standard techniques used in plunger-devices experiments.

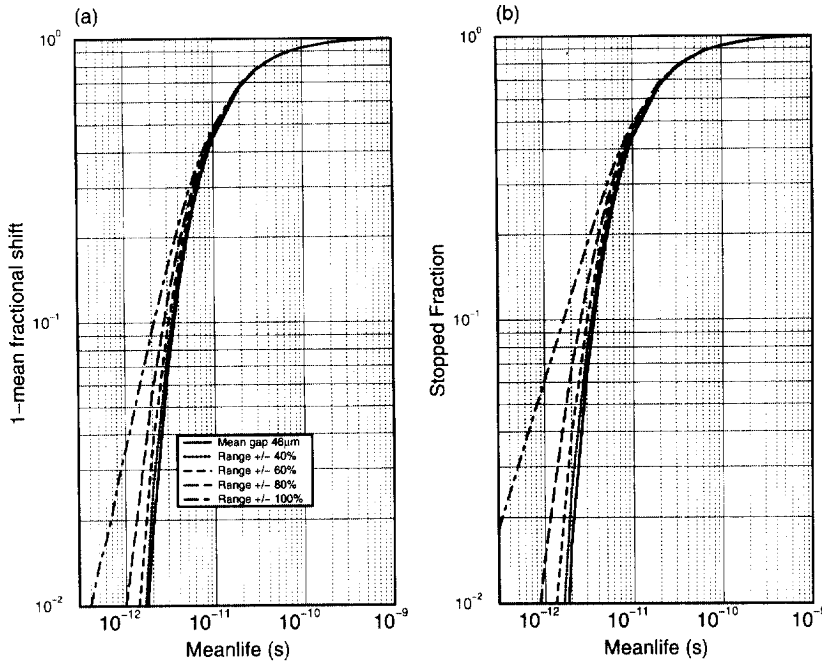

Fig. 2. Calculations of (a) the mean fractional shift and (b) the stopped fraction F versus gap range for the Coulomb excitation and (HI,xn) reaction.

4. Time-decay history of normal deformed states

In order to obtain time information for normal-deformed high-spin states in ^{193,194}Hg, gated coincidence matrices were created. For each nucleus, two matrices were sorted where information from the detectors belonging either to the 50° or to the 130° ring was stored on one axis with the other axis containing information from all other detectors in the array. These matrices were incremented with events satisfying sets of primary coincidence gates placed on transitions in either of the nuclei of interest. Only transitions not exhibiting flight fractions were chosen as gates. The primary gate set for ^{193}Hg consisted of eleven transitions below the $33/2^+$, $27/2^-$, and $25/2^-$ states in the ABC, ABF, and ABE bands (Fig. 3), respectively. For ^{194}Hg, primary gates were set on eleven transitions below the 10^+, 11^-, and 10^- level in the AB, AE and AF bands (Fig. 4), respectively. From these matrices, final spectra were generated for each band by placing secondary gates on various transitions within the respective bands as described below. Normalized total projections of the primary gated matrices served as background spectra. The stopped fractions F were determined for transitions in each of the isotopes for both the 50° and 130° rings. The measured stopped-to-total ratios were averaged, when possible, over the two rings. The results discussed below for the stopped fractions F constitute a time differential measurement for one particular value of the spacing between the ^{150}Nd and the gadolinium foil, and are presented for the three main decay sequences in both ^{193}Hg and ^{194}Hg.

4.1. ^{193}Hg

A partial level diagram and band classification scheme for ^{193}Hg are displayed in Fig. 3. Partial spectra of the ABC band, obtained in the 50° and 130° rings of detectors, are displayed in Fig. 5. The spectra were obtained by placing secondary gates on the 193.5-, 617.9- and 738.8-keV transitions in both matrices. Spectra of the ABF + ABCDF band were produced by gating on the 205.1-keV and 745.5-keV transitions while spectra of the ABE + ABCDE bands were generated by gating on the 130.5-, 375.3-, 857.7-, 885.8-, and 1000.5-keV transitions. The results, summarized in Fig. 6, display the stopped fraction $F = [\text{stopped}/(\text{stopped} + \text{flight})]$ as a function of excitation energy. The parameter F is a measure of the total elapsed time from the moment at which the nuclear reaction occurred until the decay of the particular level. For a given gap, levels with decay times longer than the flight time of 8.2 ps will exhibit mostly stopped components, while levels with much shorter decay times will exhibit mostly flight components. For illustration purposes only, the time scale on the right axis of Fig. 6 represents an approximate decay-time scale based on pure exponential decay.

An interesting feature can immediately be discerned from Fig. 6: the ABC band exhibits stopped fractions above spin $37/2^+$ smaller by a factor of about two than the stopped fractions in other bands. As an example, consider the 807.7 keV and 523.2 keV

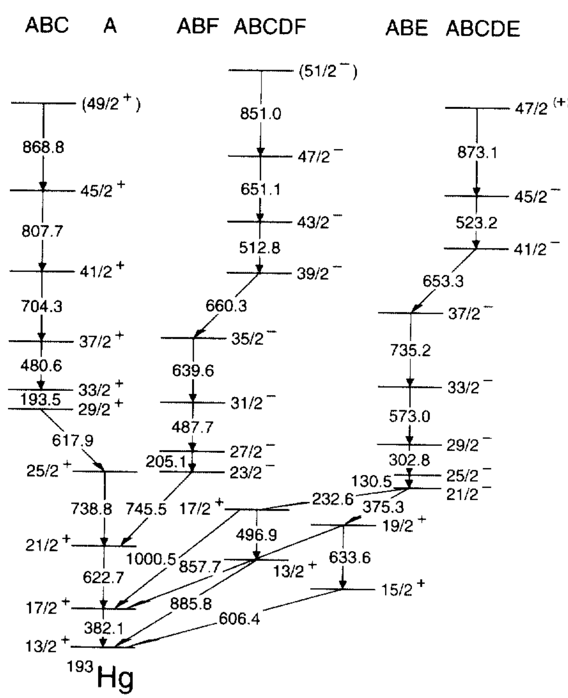

Fig. 3. Schematic band structure and classification scheme of ^{193}Hg based on Refs. [6,10]. The various bands discussed in the text are indicated.

transitions from the $45/2^+$ and $45/2^-$ in the ABC and ABCDE bands, respectively (Fig. 6). These transitions originate from states with comparable excitation energy, $\sim$ 4.5 MeV, and same spin. However, they exhibit different stopped fractions F. The *difference* in the feeding or decay times of these two bands is about 5 ps.

Recent investigations of high-spin states in Hg isotopes [10–12] highlight the existence of rather complicated irregular structures which, according to theoretical expectations, correspond to shape-changing configurations. Frequently such non-rotational structures exhibit states which decay through low-energy transitions and are relatively long-lived. These states could trap the feeding cascades populating the yrast rotational bands. For example, consider the structure which feeds mostly the ABCDE band as shown in Fig. 1 of Ref. [11]. Stopped fractions were measured for the 284.2-, 396.6-, 197.3-, 160.1-, and 357.1-keV transitions de-exciting the 5690.5-, 6322.6-, 6895.3-, 7055.4- and 7412.5-keV levels, respectively. As is indicated in Fig. 6, the transitions up to $\sim$ 7.4 MeV excitation energy exhibit stopped fractions $F \sim 0.4$, indicating a trap at even higher energies.

The lower stopped fractions of the ABC band could be explained by a weaker "trapped" feeding cascade or, alternately, by the lower excitation energy at which a delayed cascade feeds the band. This reasoning might explain the steep rise of the stopped component below the $41/2^+$, 3739.9-keV level. The present lack of high-spin spectroscopic information precludes further discussion of the above hypotheses.

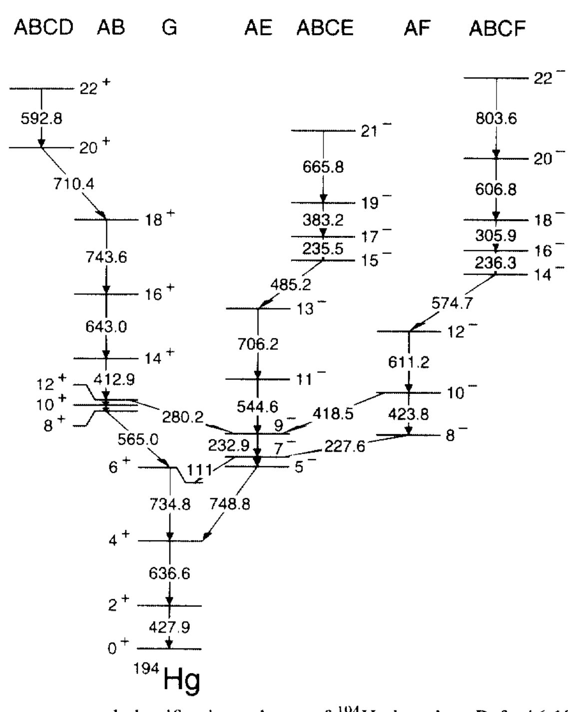

Fig. 4. Schematic band structure and classification scheme of ^{194}Hg based on Refs. [6,10]. The various bands discussed in the text are indicated.

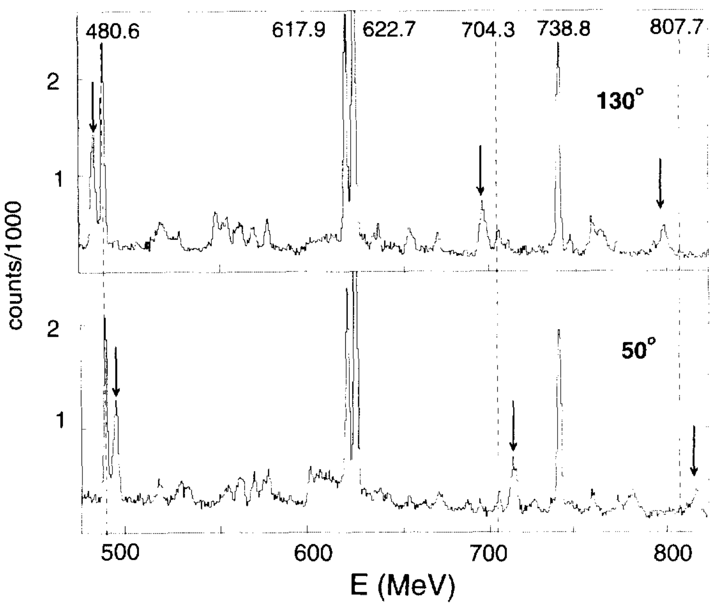

Fig. 5. Comparison of partial spectra for the ABC band of ^{193}Hg in backward (130°) and forward (50°) rings of Gammasphere. The dashed vertical lines indicate the energies of the stopped peaks. Energies are given in keV.

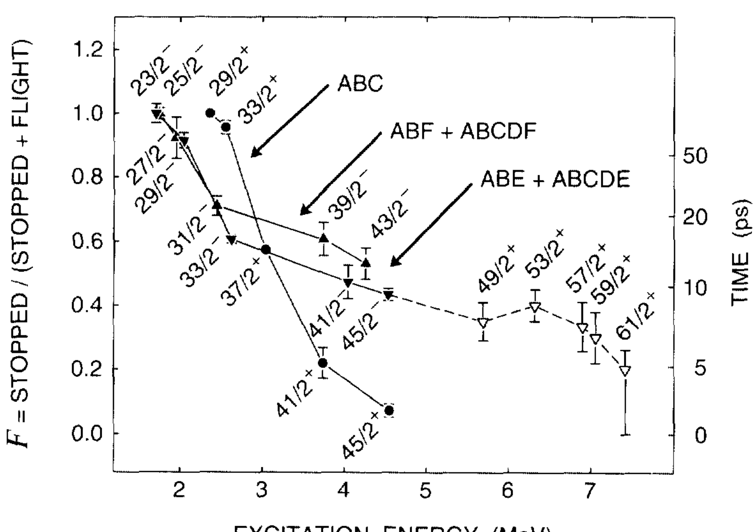

Fig. 6. Measured stopped fraction F presented as function of excitation energy for three bands in ^{193}Hg. The time scale on the right axis corresponds to a pure exponential decay and is presented for illustration purposes only. The data points belonging to transitions within a particular band are connected by lines.

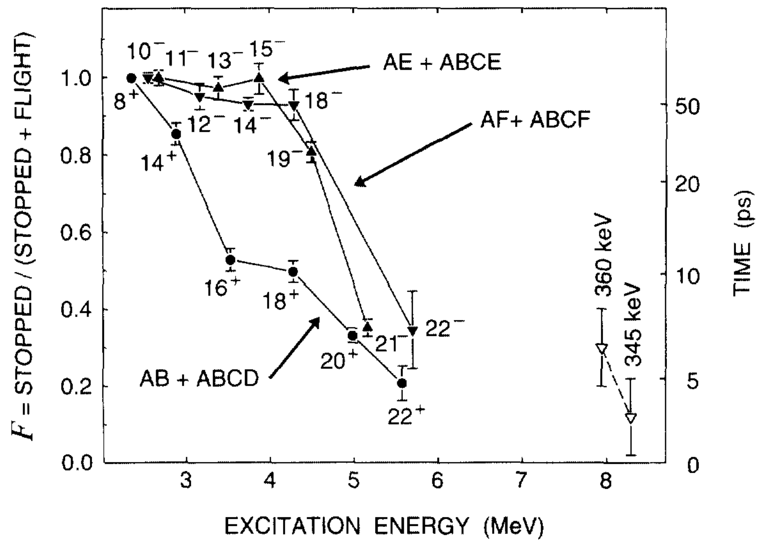

Fig. 7. Measured stopped fraction F as function of excitation energy for various normal-deformation bands in ^{194}Hg. The time scale on the right axis corresponds to a pure exponential decay and is presented for illustration purposes only.

4.2. ^{194}Hg

A similar analysis has been applied to study the time history of normal-deformed bands in ^{194}Hg. A partial level diagram and band classification scheme are displayed in Fig. 4. The two spectra for the forward and backward rings of the AB + ABCD band in ^{194}Hg were produced by gating on the 734.8-keV and 565.0-keV transitions. The spectra of the AE + ABCE band were obtained by gating on the 748.8-, 232.9- and 544.6-keV transitions and the spectra of the AF + ABCF band by gating on the 748.8-, 227.6-, 418.5- and 423.8-keV lines. The results of the stopped fraction measurements are shown in Fig. 7. The results for two new transitions, 359.8 keV de-exciting the 7941.3-keV level and 345.4 keV de-exciting the 8287.3-keV level (labeled as structure "2" in Ref. [10]), are also presented. The stopped components of ^{194}Hg transitions are larger, in general, than those of ^{193}Hg at the corresponding excitation energy. This effect may reflect a lower entry point for the 5n channel, and consequently, a shorter decay cascade.

As in the case of ^{193}Hg,some bands in ^{194}Hg exhibit different time-decay histories. The AB + ABCD band has a short feeding time, while the AE + ABCE and AF + ABCF bands exhibit a larger stopped fraction, below ~ 5 MeV excitation energy. The delay in the transitions up to the 15^- state in the ABCE band and 18^- in the ABCF band may be due to long-lived states at the second backbendings at 4114.7 keV and 3983.4 keV de-excited by transitions of 235.5 keV and 236.3 keV, respectively. The delay in the 18^- state can be attributed to delayed feeding from higher, yet unplaced transitions. Similar conclusions apply to the fast 21^- and the slower 19^- states in the

ABCE band. Several new weaker transitions [21] at 437, 542, 688, 779, 898, 921 and 934 keV as well as transitions at 146 and 532 keV mentioned previously by Hübel et al. [6] have been observed in a band at around 9 MeV which feeds both the ABCE and the ABCF bands. None of these transitions could be placed in the level scheme. The three transitions at 779, 688, and 921 keV were found to feed the 18^- state. In addition, previously observed [6] transitions, at 315 keV and 460 keV were seen to be fully shifted, while the 253-, and 227-keV transitions were partially shifted.

More detailed spectroscopic information regarding these levels is needed in order to obtain a more comprehensive picture.

5. Discussion

There has been much interest in the study of high spin, normal deformed, states in this mass region. In particular, rotational bands built on a large number of quasiparticle configurations have been identified at high spin and excitation energies in ^{193,194}Hg as well as many single particle excitations connected to rotational bands by complex decay patterns [6–12]. In the present experiment, new high-excitation, fully or partially shifted, and previously unplaced transitions, were observed for ^{194}Hg.

The measurements of line shapes of high-spin states in normal deformed states have shown that different low-lying rotational bands in the same nucleus can have different feeding times. Also, ^{193}Hg and ^{194}Hg differ, in general, in a manner consistent with the lower entry point of the 5n compared to the 4n channel. Further experimental information regarding the entry point distribution for the present reaction and energy is needed to correlate this qualitative observation to detailed Monte Carlo simulations.

One of the fascinating results of the present analysis of the yrast and near yrast transitions in ^{193,194}Hg relates to the presence of sidefeeding into the yrast states with rather long lifetimes, i.e. with lifetimes on the order of a few picoseconds. It appears that at least a fraction of the states which populate the yrast levels are non-collective in nature. The situation has similarities with that observed in the beginning of the rare earth region, in particular in the light Dy isotopes. For example, as spin increases along the ^{154}Dy yrast line, the level spacing characteristic of a rotational sequence associated with a moderate prolate deformation ($\beta_2 \sim 0.2$, $\gamma = 0°$) gives way to a level structure (at $I \sim 30\hbar$) which is much more irregular in energy [22]. This sequence of states represents a gradual transition from a prolate to an oblate shape which theory describes in terms of band termination [23], a process where under the stress of rotation the spins of several pairs of nucleons gradually align with the nuclear symmetry axis until the maximally aligned or terminating state is reached. Lifetime measurements by Azgui et al. [24] for the collective yrast states ($I \leqslant 30\hbar$) in ^{154}Dy indicate that the sidefeeding into these states is characterized by both a fast ($\leqslant 1$ ps) and a slow (~ 10 ps) component. The intensity of the slow component was found to increase with angular momentum. These observations indicate that the yrast levels are fed both through collective states and through configurations of aligned-particle character similar to those seen at the highest spins along the yrast line. In other words, the prolate to oblate shape transition alluded to above manifests itself above the yrast line as well. In the beginning of the rare earth region, the generation of angular momentum by the alignment of the spins of nucleons along the symmetry axis results in an oblate, non-collective shape where the shape-polarizing effects are provided by *particles* occupying high-j orbitals ($\nu i_{13/2}$, $\pi h_{11/2}$, etc.).

As was first shown by Ye at al. [7], the same mechanism of "non-collective" angular momentum generation also occurs in the Hg nuclei. These nuclei, which are characterized by a moderate oblate-collective shape ($\beta_2 \sim 0.2$, $\gamma = -60°$), undergo a shape change towards a prolate non-collective ($\gamma = -120°$) shape at higher spin for which the driving force is provided by *holes* in the same high-j orbitals which are responsible for the oblate non-collective shape in the Dy isotopes. As was shown in Refs. [7,25], Nilsson-Strutinsky calculations indicate the following general features for the Hg nuclei: (1) for spins I = 20-30$\hbar$, two minima are present in the energy surfaces corresponding to collective near-oblate configurations ($\beta_2 h \sim 0.2$, $\gamma = -40°$) and to aligned prolate non-collective configurations ($\beta_2 \sim 0.1$-0.15, $\gamma = -120°$), respectively; (2) the prolate non-collective configurations become favored energetically for $I > 30\hbar$; at spin $I \sim 40\hbar$, the valence space is essentially exhausted and a third minimum at $\beta_2 = 0.2$-0.3, $\gamma \sim 20°$ (involving $h_{9/2}$ and $i_{13/2}$ protons) becomes energetically competitive; (3) a superdeformed minimum is present at all spins with $\beta_2 \sim 0.5$ and $\gamma = 0°$ and becomes yrast at $I \sim 40\hbar$. The present time-decay history data suggest that the analogy between the structure of A = 150 and A = 190 nuclei extends beyond the yrast levels to the feeding states, i.e. the sidefeeding is characterized not only by collective transitions, but also by γ-ray flux associated with decay from non-collective configurations.

Acknowledgements

We would like to acknowledge the target preparation by Mr. Leo Sapir of the Weizmann Institute and the help of the technical staff at the Berkeley 88" Cyclotron.

This work was supported in part by the Binational Israel-U.S. Science Foundation (BSF), the U.S. National Science Foundation and the U.S. Department of Energy under contract numbers W-31-109-ENG-38 (ANL) and DE-ACO3-76SF00098 (LBL).

References

[1] R.V.F. Janssens and T.L. Khoo, Ann. Rev. Nucl. Part. Sci. 41 (1991) 321.

[2] E.F. Moore, R.V.F. Janssens, I. Ahmad, M.P. Carpenter, P.B. Fernandez, T.L. Khoo, S.L. Ridley, F.L.H. Wolfs, D. Ye, K.B. Beard, U. Garg, M.W. Drigert, Ph. Benet, P.J. Daly and R. Wyss, Phys. Rev. Lett. 64 (1990) 3127.

[3] A. Korichi, F. Hannachi, I. Deloncle, W. Korten, I. Ahmad, F. Azaiez, G. Bastin, C.W. Beausang, C. Bourgeois, M.P. Carpenter, R.M. Clark, R. Duffait, J. Duprat, B.J.P. Gall, R.G. Henry, H. Hübel, R.V.F. Janssens, M.J. Joyce, M. Kaci, T.L. Khoo, T. Lauritsen, Y. Le Coz, M. Meyer, E.S. Paul, N. Perrin, N. Poffé, M.G. Porquet, N. Redon, C. Schück, H. Sergolle, J.F. Sharpey-Schafer, J. Simpson, A.G. Smith, R. Wadsworth and P. Willsau, Phys. Lett. B 345 (1995) 403.

[4] R. Kühn, A. Dewald, R. Krücken, C. Meier, R. Peusquens, H. Tiesler, O. Vogel, S. Kosemann, P. von Brentano, D. Bazzacco, C. Rossi-Alvarez, S. Lunardi and J. de Boer, Phys. Rev. 55 (1997) 1002.
[5] T.L. Khoo, M.P. Carpenter, T. Lauritsen, D. Ackermann, I. Ahmad, D.J. Blumenthal, S.M. Fisher, R.V.F. Janssens, D. Nisius, E.F. Moore, A. Lopez-Martens, T. Dössing, R. Krücken, S.J. Asztalos, J.A. Becker, L. Bernstein, R.M. Clark,M.A. Deleplanque, R.M. Diamond, P. Fallon, L.P. Farris, F. Hannachi, E.A. Henry, A. Korichi, I.Y. Lee, A.O. Macchiavelli and F.S. Stephens, Phys. Rev. Lett. 76 (1996) 1583.
[6] H. Hübel, A.P. Byrne, S. Ogaza, A.E. Stuchbery, G.D. Dracoulis and M. Guttormsen, Nucl. Phys. A 453 (1986) 316.
[7] D. Ye, R.V.F. Janssens, M.P. Carpenter, E.F. Moore, I. Ahmad, K.B. Beard, Ph. Benet, M.W. Drigert, U. Garg, Z.W. Grabowski, T.L. Khoo, F.L.H. Wolfs, T. Bengtsson and I. Ragnarsson, Phys. Lett. B 236 (1990) 7.
[8] D. Ye, K.B. Beard, U. Garg, R.V.F. Janssens, M.P. Carpenter, I. Ahmad, T.L. Khoo, E.F. Moore, F.L.H. Wolfs, Ph. Benet, Z.W. Grabowski and M.W. Drigert, Nucl. Phys. A 537 (1992) 207.
[9] I.G. Bearden, R.V.F. Janssens, M.P. Carpenter, E.F. Moore, I. Ahmad, P.J. Daly, R.H. Mayer, M.W. Drigert, P.B. Fernandez, B. Fornal, U. Garg, Z.W. Grabowski, T.L. Khoo, T. Lauritsen, W. Reviol and D. Ye, Nucl. Phys. A 576 (1994) 441.
[10] J.K. Deng, W.C. Ma, J.H. Hamilton, J.D. Garrett, C. Baktash, D.M. Cullen, N.R. Johnson, I.Y. Lee, F.K. McGowan, S. Pilotte, C.H. Yu and W. Nazarewicz, Phys. Lett. B 319 (1993) 63.
[11] N. Fotiades, S. Harissopulos, C.A. Kalfas, S. Kossionides, C.T. Papadopoulos, R. Vlastou, M. Serris, M. Meyer, N. Redon, R. Duffait, Y. Le Coz, L. Ducroux, F. Hannachi, I. Deloncle, B. Gall, M.G. Porquet, C. Schück, F. Azaiez, J. Duprat, A. Korichi, J.F. Sharpey-Schafer, M.J. Joyce, C.W. Beausang, P.J. Dagnall, P.D. Forsyth, S.J. Gale, P.M. Jones, E.S. Paul, J. Simpson, R.M. Clark, K. Hauschild and R. Wadsworth, J. Phys. G 21 (1995) 911.
[12] N. Fotiades, S. Harissopoulos, C.A. Kalfas, S. Kossionides, C.T. Papadopoulos, R. Vlastou, M. Serris, J.F. Sharpey-Shafer, M.J. Joyce, C.W. Beausang, P.J. Dagnall, P.D. Forsyth, S.J. Gale, P.M. Jones, E.S. Paul, P.J. Twin, J. Simpson, D.M. Cullen, P. Fallon, M.A. Riley, R.M. Clark, K. Hauschild and R. Wadsworth, Z. Phys. A 354 (1996) 169.
[13] P. Willsau, M. Neffgen, Y. Le Coz, H. Hübel, W. Korten, F. Hannachi, A. Korichi. M.G. Porquet, M. Kaci, N. Redon, M. Meyer, C.W. Beausang, E.S. Paul, J. Simpson and J.R. Hughes, Z. Phys. A 355 (1996) 129.
[14] I.Y. Lee, Nucl. Phys. A 520 (1990) 641c.
[15] M. Hass, J.M. Brennan, H.T. King, T.K. Saylor and R. Kalish, Phys. Rev. C 14 (1976) 2119.
[16] C.W. Beausang, D. Prevost, M.H. Bergstrom, G. deFrance, B. Haas, J.C. Lisle, Ch. Theisen, J. Timár, P.J. Twin, J.N. Wilson, Nucl. Instrum. Methods Phys. Res. A 364 (1995) 560.
[17] B. Crowell, M.P. Carpenter, R.G. Henry, R.V.F. Janssens, T.L. Khoo, T. Lauritsen and D. Nisius, Nucl. Instrum. Methods Phys. Res. A 355 (1995) 575.
[18] Average of the meanlives from S.W. Yates, N.R. Johnson, L.L. Riedinger and A.C. Kahler, Phys. Rev. C 17 (1978) 634;
D. Cline, private communication.
[19] J.F. Ziegler, J.P. Biersack and U. Littmark, The Stopping and Range of Ions in Solids (Pergamon, New York, 1985);
J.F. Ziegler, private communication (1995).
[20] M.W. Guidry, P.A. Butler, R. Donangelo, E. Grosse, Y. El Masri, I.Y. Lee, F.S. Stephens, R.M. Diamond, L.L. Riedinger, C.R. Bingham, A.C. Kahler, J.A. Vrba, E.L. Robinson and N.R. Johnson, Phys. Rev. Lett. 40 (1978) 1016; R. Bass, *in* Nuclear Reactions with Heavy Ions (Springer, Berlin, 1980) p. 76.
[21] These transitions were observed in a later experiment with a gapless target, R.H. Mayer, L. Weissman, N. Benczer-Koller, C. Broude, J.A. Cizewski, M. Hass, J. Holden, R.V.F. Janssens, G. Kumbartzki, T. Lauritsen, I.Y. Lee, A.O. Macchiavelli, N. Matt, D.P. McNabb and M. Satteson (to be published).
[22] W.C. Ma, M.A. Quader, H. Emling, T.L. Khoo, I. Ahmad, P.J. Daly, B.K. Dichter, M. Drigert, U. Garg, Z.W. Grabowski, R. Holzmann, R.V.F. Janssens, M. Piiparinen, W.H. Trzaska and T.-F. Wang, Phys. Rev. Lett. 61 (1988) 46.
[23] T. Bengtsson and I. Ragnarsson, Physica Scripta T5 (1983) 165.
[24] F. Azgui, H. Emling, E. Grosse, C. Michel, R.S. Simon, W. Spreng, H.J. Wollersheim, T.L. Khoo, P. Chowdhury, D. Frekers, R.V.F. Janssens, A. Pakkanen, P.J. Daly, M. Kortelahti, D. Schwalm and G. Seiler-Clark, Nucl. Phys. A 439 (1985) 573.
[25] I. Ragnarsson, T. Bengtsson, G. Leander and S. Åberg, Nucl. Phys. A 347 (1980) 287.